

Light Scattering Study of Poly(phenylhydroquinone-co-terephthalic acid)

William R. Krigbaum and Takumi Tanaka*

Department of Chemistry, Duke University, Durham, North Carolina 27706.
Received June 29, 1987; Revised Manuscript Received September 3, 1987

ABSTRACT: The wholly aromatic polyester, poly(phenylhydroquinone-co-terephthalic acid), first disclosed in the Payet patent,¹ is studied by differential scanning calorimetry and dilute solutions of fractions are examined by static and dynamic light scattering techniques. This polyester has two crystal modifications and exhibits a thermotropic nematic phase over the temperature range 350–450 °C. The intrinsic viscosity (dL/g) measured at 25 °C in a 50:50 mixture by weight of *o*-dichlorobenzene and *p*-chlorophenol is related to the molecular weight by $[\eta] = 3.0 \times 10^{-4} (M_w)^{0.869}$. Values for the persistence length calculated by three methods range from 60 to 150 Å, with an average of 100 Å. Space-filling models indicate that the substituent phenyl group prevents the benzene ring and the adjacent carbonyl group from being planar. This may offer an explanation for the small persistence length. Nevertheless, a persistence length of 100 Å is smaller than expected for a thermotropic polymer having a nematic-isotropic transition temperature of 450 °C.

Introduction

Since Kevlar was patented almost 15 years ago, a number of rigid and semirigid polymers have been developed which exhibit a nematic phase in solution or in the melt. Some of these have been commercialized. Their mechanical properties in the form of fibers or films are significant for reinforced materials. It is important to determine the chain conformations of these polymers. Fortunately, the wormlike chain model of Kratky and Porod² yields a parameter, the persistence length, which quantifies the chain extension of this class of semirigid polymer molecules. For a Gaussian chain, such as polystyrene, the persistence length is about 10 Å. For the semirigid polymers the persistence length is larger by an order of magnitude, or more. Several papers have reported the persistence length of Kevlar,^{3–6} the polyterephthalamide of *p*-aminobenzhydrazide,^{7–11} cellulose and various cellulose derivatives,¹² and poly(γ -benzyl-L-glutamate).^{13,14} In this paper we examine the polyester poly(phenyl *p*-phenylene terephthalate), first disclosed by Payet.¹ The fiber properties of this polymer, reported by Payet¹ and by Jackson,¹⁵ are excellent after the fibers are heat treated according to the process disclosed by Luise.¹⁶ The persistence length was estimated according to several theories by using viscosity and static and dynamic light scattering measurements. The thermal transitions of the polymer sample prepared in this laboratory are also described.

Experimental Section

Differential scanning calorimeter data were obtained by using a Du Pont 1090 DSC. The light scattering instrument consisted of a 35-mW Spectra Physics Model 127 He-Ne laser, an automated Picker goniometer, a Malvern K7025 Multibit Correlator, and a Malvern photomultiplier assembly holding an ITT FW130 photomultiplier.

Static light scattering measurements were first attempted with an argon ion laser using 514.5-nm green light. However, the polymer solutions exhibited fluorescence and absorbed at this wavelength. The fluorescence could be overcome by a narrow-band-pass filter; however, absorbance caused the incident beam to spread due to heating and a change in the refractive index. Therefore, a longer wavelength He-Ne laser giving a 632.8-nm red light was chosen for these measurements. Since the Spectra Physics Model 127 produces horizontally polarized light, it was necessary to introduce a mica half-wave plate to obtain vertically polarized light. The incident beam passes through a 15-cm focal length lens and into a vat filled with xylenes (refractive index 1.49)

which contains a beam stop. An analyzer is mounted in front of the photomultiplier so that either vertical or horizontal scattered light can be measured. The photomultiplier has a 1-mm aperture for static measurements and a 632.8-nm narrow-band-pass filter. A sample cell 12 mm in diameter was tried, but reflection effects limited the reliable angular range to 50–120°. Better results were obtained with a sample tube 16 mm in diameter, which permitted measurements over the angular range 30–135°.

One would prefer to use a single solvent for light scattering measurements. Lenz¹⁷ has given a table of solvents for aromatic polyesters. However, wholly aromatic polyesters have only limited solubility, and no single solvent for this polymer was found. If one must resort to a mixed solvent, the two liquids must have nearly the same refractive indices. A mixed solvent consisting of 50:50 by weight of *o*-dichlorobenzene and *p*-chlorophenol was selected to meet this criterion. HPLC grade *o*-dichlorobenzene was used as received from Aldrich; however, the *p*-chlorophenol from Aldrich had to be distilled because its color was brown. The two viscometer constants were determined by measuring the flow times of benzene and water. The density of the mixed solvent at 25 °C is 1.300 g/mL and its viscosity is 3.468 cP. The refractive index of the mixed solvent is 1.55. The refractive index increment was measured at 632.8 nm by using a Brice-Phoenix refractometer.¹⁸ Due to the high refractive index of the mixed solvent, the image of the slit could not be seen in the Brice-Phoenix refractometer. It was necessary to rotate the cell and to calibrate the instrument at this fixed position. The refractive index increment is 0.0742, as determined from the data shown in Figure 1.

For dynamic measurements the aperture was reduced to 0.5 mm and the angular range was 20–135°. The number of coherence areas, n_{coh} should be less than unity. n_{coh} is equal to the ratio of the area of the aperture divided by the coherence area, A_{coh} . Ford¹⁹ gives the following relation for the coherence area:

$$A_{\text{coh}} = \lambda_0^2 R^2 / \pi a^2 \quad (1)$$

where λ_0 is the wavelength in vacuo, R is the distance from the scattering volume to the detector, and a is the radius of the scattering volume (or the radius of the laser beam at the point where the scattering is measured). According to Chu,²⁰ the diameter of the laser beam at the focal length, f , of the lens is given by

$$2a = 4\lambda_0 f / \pi D \quad (2)$$

where D is the diameter of the laser beam before the lens. In our case f , D , λ_0 , and R are 15 cm, 0.125 cm, 632.8 nm, and 11 cm, respectively. From eq 1 and 2 we obtain $A_{\text{coh}} = 6.6 \times 10^{-3} \text{ cm}^2$. The area of the aperture for a 0.5-mm-diameter pinhole is $1.96 \times 10^{-3} \text{ cm}^2$, so $n_{\text{coh}} = 0.297$.

Results

1. Monomers, Polymerization, and Fractionation. Terephthalic acid of high purity (99.99%) was used as received from Du Pont. It was dried overnight in a vacuum

* Permanent address: Unitika Ltd., 23 Kozakura, Uji, Kyoto 611, Japan.

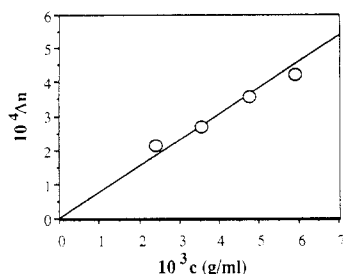


Figure 1. Refractive index increment versus concentration for fraction F4.

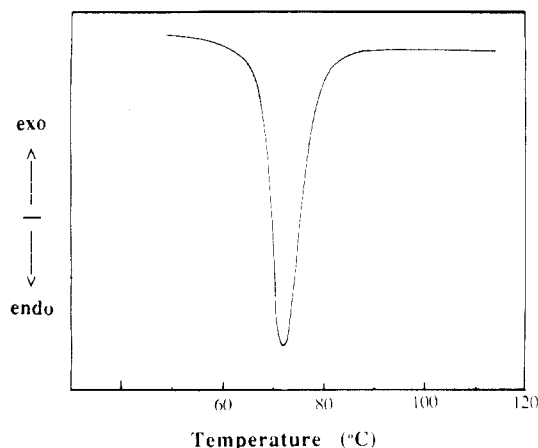


Figure 2. DSC heating curve for the diacetate of phenylhydroquinone.

Table I
Steps in Polymerization

step	t , °C	p , atm	time, h
1	285	1	1.0
2	304	1	1.0
3	350	1	1.0
4	350	vacuum	0.75

oven at 30 °C. Phenylhydroquinone was purified by stirring a dilute ethanol solution with a small amount of carbon black for 3 days and then filtering. An equivalent volume of water was added, and the liquid was cooled with ice and kept overnight. Filtration yielded a white precipitate of phenylhydroquinone. This purified product was refluxed at 110 °C for 1 day with excess acetic anhydride. The unreacted acetic anhydride was distilled off and the product was dissolved in ethanol. An equal volume of hexane was added and the liquid was cooled with ice and kept overnight. After the white crystals of the diacetate were filtered, they were dried overnight at 30 °C in a vacuum oven. As indicated by the DSC curve shown in Figure 2, the melting temperature of the diacetate was 68–70 °C.

A very small amount of Mg metal as a catalyst was added to 0.025 mol (4.2 g) of terephthalic acid and 0.026 mol (7.0 g) of phenylhydroquinone diacetate. This mixture was transferred to a tube on a vacuum line and the tube was alternately evacuated and filled with argon to remove oxygen completely. The polymerization was carried out in four steps, as indicated in Table I. A steady stream of argon gas was used in the first three steps. The resulting polymer was light green in color. Its inherent viscosity, as measured at 25 °C in a 50:50 mixture by weight of *o*-dichlorobenzene and *p*-chlorophenol, was 2.66 dL/g.

Seven grams of polymer were dissolved in 5 L of the mixed solvent at 23 °C and methanol was added dropwise until the solution became turbid. The two-phase system was heated to 100 °C until it became clear, and then the

Table II
Characterization of Fractions

fraction	$[\eta]$, dL/g	k	$-k'$
F1	3.500	0.363	0.136
F2	3.330	0.372	0.131
F3	2.418	0.369	0.131
F4	1.912	0.373	0.128
F5	1.810	0.369	0.130
F6	1.455	0.371	0.128
F7	1.113	0.371	0.129
F8	0.861	0.337	0.126
F9	0.587	0.369	0.138

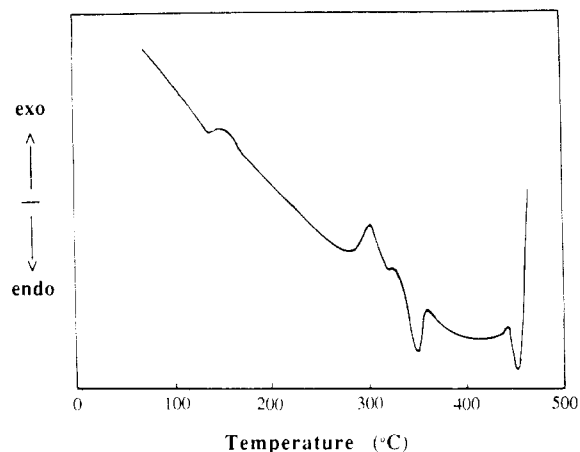


Figure 3. First DSC heating curve of poly(phenyl *p*-phenylene terephthalate) fraction F4.

solution was placed in the 23 °C water bath and allowed to stand overnight. The sol and gel phases were separated by centrifugation and the gel phase was precipitated by pouring it into methanol with rapid stirring in a blender. The precipitate was filtered and dried completely in a vacuum oven at 100 °C. This procedure was repeated until nine fractions were obtained. These were characterized by measuring their intrinsic viscosities. These data, along with the Huggins constants k and k' , are given in Table II. The value of $k - k'$ is nearly 0.5 for all of the fractions.

2. Thermal Transitions. The thermal transitions were studied by using small samples of fraction F4. Figure 3 shows the first DSC heating curve of this sample over a wide temperature range taken at a rate of 10 °C/min. The glass transition appears at 140 °C, which is lower than the 170 °C value reported by Krigbaum, Hakemi, and Kotek.²¹ An exotherm representing crystallization occurs at 300 °C, and the crystal–nematic transition appears at 350 °C upon first heating. The endotherm at 455 °C represents the nematic–isotropic transition. The isotropic phase is not stable at higher temperatures, as indicated by the sharp rise in the curve following this endotherm. The nematic phase was observed in the polarizing microscope equipped with a hot stage from 360 to 460 °C. The field of view became dark above 460 °C, indicating a transition to the isotropic phase. Figure 4 shows the heating curve of a second sample over a shorter temperature interval, 240–370 °C. Crystallization and melting occur at somewhat lower temperatures, 293 and 343 °C. The lower curve in Figure 4 represents a cooling curve taken at 5 °C/min. A sharp crystallization exotherm is seen at 300 °C. This sample was slowly cooled to room temperature and heated a second time. The second heating curve, shown in Figure 5, exhibits two endotherms at about 320 and 340 °C. This indicates that heat treatment produces two crystalline polymorphs. These stand in reasonable agreement with the values 320 and 346 °C reported by Krigbaum, Hakemi, and Kotek²¹ for the same polymer. The second cooling

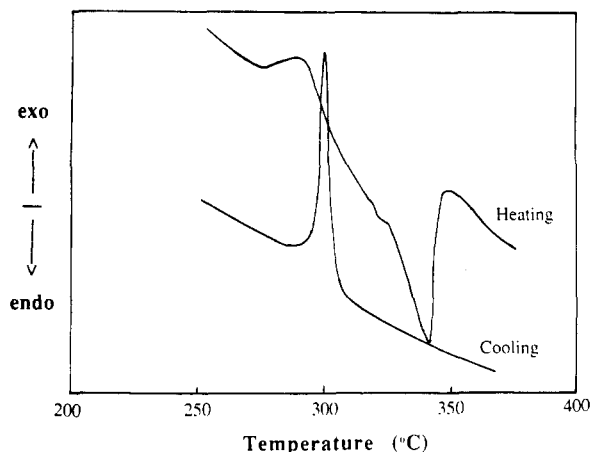


Figure 4. First DSC heating and cooling curves for fraction F4 over a more limited temperature range.

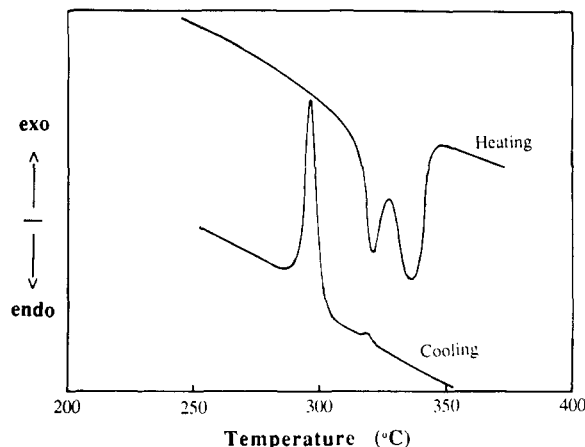


Figure 5. Second heating and cooling curves of fraction F4. curve is similar to the first except for a small exotherm at 320 °C.

3. Static Light Scattering. The light scattering data are expressed in terms of Rayleigh's ratio, which is defined for unpolarized light as²²

$$R_u(\theta) = i(\theta)r^2/(I_0V) \quad (3)$$

Here $i(\theta)$ is the excess intensity scattered at angle θ as measured at a distance r from the irradiated volume V of the solution, while I_0 is the irradiance of the incident light. Rayleigh's ratio is normally determined by comparison with the scattering of a standard. When toluene is chosen as the standard, Rayleigh's ratio is given by

$$R_u(\theta) = (n_s/n_v)^2 [\Delta I_p/I_t(\pi/2)] R_{u,t}(\pi/2) \sin(\theta)/(1 + \cos^2 \theta) \quad (4)$$

Here n_s and n_v are the refractive indices of the solvent and the liquid in the vat, ΔI_p is the excess scattering intensity of the polymer solution at angle θ , and $I_t(\pi/2)$ is the scattered intensity and $R_{u,t}(\pi/2)$ is the Rayleigh ratio of toluene, both at 90°. If the incident and scattered light are both vertically polarized, this relation becomes

$$R_{vv}(\theta) = (n_s/n_v)^2 [\Delta I_p/I_t(\pi/2)] R_{vv,t}(\pi/2) \sin \theta \quad (5)$$

Values of $R_u(\pi/2)$ for toluene at 632.8 nm were given by Kaye and Havlik²³ and by Pike, Pomeroy, and Vaughan.²⁴ These values were averaged. The depolarization ratio of toluene is $\rho_u = 0.48$. This value along with the average value of $R_u(\pi/2)$ for toluene at 632.8 nm was used to obtain $10^5 R_{vv}(\pi/2) = 10.7$ from the relation given by Nagai:²⁵

$$R_{vv}(\pi/2) = [(2 - \rho_u)/(1 + \rho_u)] R_u(\pi/2) \quad (6)$$

According to the treatment of Zimm²⁶

$$Kc/R_{vv}(\theta, c) = (1/\langle M \rangle_w + 2A_2c)/P(\theta) \quad (7)$$

where $K = 4\pi^2 n^2 (dn/dc)^2 / \lambda_0^4 N_A$. Here n is the refractive index of the solvent, dn/dc is the refractive index increment, and N_A is Avogadro's number. In this equation $\langle M \rangle_w$ is the weight-average molecular weight, A_2 is the second virial coefficient, and

$$1/P(\theta) = 1 + (16\pi^2/3\lambda^2) \langle s^2 \rangle_z \sin^2(\theta/2) \quad (8)$$

where $\langle s^2 \rangle_z$ is the z -average mean-square radius of gyration and $\lambda = \lambda_0/n$ is the wavelength in the medium having refractive index n . By making the Zimm plot,²⁶ one obtains values of $\langle M \rangle_w$, $\langle s^2 \rangle_z$, and A_2 . However, if there is depolarization, all these values must be considered apparent. The depolarization ratio, ρ_v , is equal to $3\delta/(4\delta + 1)$. Hence the anisotropy, δ , is given by

$$\delta = \rho_v/(3 - 4\rho_v) \quad (9)$$

Utiyama²⁷ has obtained the following modification of eq 7 for solutions with depolarization:

$$R_{vv}(\theta, c)/Kc\langle M \rangle_w = 4\delta + P(\theta) - 2A_2\langle M \rangle_w P_2(\theta)c + \dots \quad (10)$$

and

$$R_{vh}(\theta, c)/Kc\langle M \rangle_w = 3\delta \quad (11)$$

so that

$$[Kc/R_{vv}(\theta, c)]_{c=0} = [1 + P(\theta)/(4\delta + 1)]/[(4\delta + 1)\langle M \rangle_w] \quad (12)$$

and

$$[Kc/R_{vv}(0, c)] = [1 + 2A_2c/(4\delta + 1)]/[(4\delta + 1)\langle M \rangle_w] \quad (13)$$

Hence, one obtains the following relations:

$$\langle M \rangle_w = M_{app}/(4\delta + 1) \quad (14)$$

$$\langle s^2 \rangle_z = \langle s^2 \rangle_{app}(4\delta + 1) \quad (15)$$

$$A_2 = A_{2,app}(4\delta + 1)^2 \quad (16)$$

Nagai²⁵ has developed the following relations for the wormlike chain with depolarization:

$$R_{vv}(\theta, c)/Kc\langle M \rangle_w = (8/135)(\epsilon^2/X)g_2 + (4/135)q^2\epsilon k^2 g_3 + [1 - (qL/9)k^2 g_1] \quad (17)$$

$$R_{vh}(\theta, c) = (2/45)(\epsilon^2/X)g_2 - \dots \quad (18)$$

Here ϵ is the molecular anisotropy, k is the reciprocal lattice vector having the magnitude $k = (4\pi/\lambda) \sin(\theta/2)$, and $X = L/q$ is the ratio of the contour length to the persistence length. The function $g_i(X)$ can be found in Nagai's paper.²⁵

Berry²⁸ has developed corrections to the values derived from the Zimm plot which utilize the parameter $\delta_B^2 = (2/27)(\epsilon^2/X)g_2$. His relations are

$$(R_{vv}/Kc\langle M \rangle_w)_{c=0} = 1 + 4\delta_B^2/5 - [1 - 4f_1\delta_B/5 + 4(f_2\delta_B)^2/7]/(k^2/3) \quad (19)$$

$$(R_{vh}/Kc\langle M \rangle_w)_{\theta=0} = 3\delta_B^2/5 - 9(f_3\delta_B)^2 k^2/35 \quad (20)$$

where f_i is a function of L/q . From these relations one obtains

$$\langle M \rangle_w = M_{app}/(1 + 4\delta_B^2/5) \quad (21)$$

$$\langle s^2 \rangle_z = \langle s^2 \rangle_{z,app} [1 + 4\delta_B^2/5] / [1 - 4f_1\delta_B/5 + 4(f_2\delta_B)^2/7] \quad (22)$$

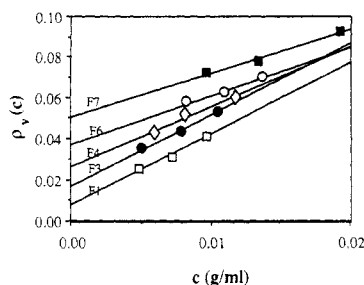


Figure 6. Concentration dependence of the depolarization ratio, ρ_v , for five fractions.

Table III
Static Light Scattering Results

	fraction				
	F1	F3	F4	F6	F7
$\langle M \rangle_{w,app}$	49 500	32 790	27 030	19 340	16 450
δ_B^2 and δ	47 790	30 680	24 080	16 600	13 070
Y	47 330	30 290	23 920	16 460	12 950
$\langle s^2 \rangle_{z,app}, nm^2$	784	551	377	307	225
δ_B^2	840	626	463	407	331
δ	812	589	423	358	283
Y	628	463	346	286	212
$10^3 A_{2,app}$	2.53	2.02	2.07	1.73	1.75
δ_B^2	2.62	2.16	2.32	2.02	2.20
δ	2.71	2.31	2.61	2.35	2.77
δ_B^2	0.045	0.086	0.153	0.207	0.323
δ	0.212	0.293	0.391	0.455	0.568

A correction to A_2 is not mentioned in Berry's paper, but A_2 can be estimated as follows:

$$A_2 = A_{2,app}(1 + 4\delta_B^2/5)^2 \quad (23)$$

Since $\rho_v = 3\delta_B^2/(4\delta_B^2 + 5)$, one can calculate δ_B^2 from the following relation:

$$\delta_B^2 = 5\rho_v/(3 - 4\rho_v) \quad (24)$$

This indicates Berry's δ_B^2 is equivalent to Utiyama's 5δ . Values for δ_B^2 and δ are listed at the bottom of Table III.

Utiyama²⁷ and Nagai²⁵ have suggested that the corrected molecular weight and mean-square radius of gyration can be obtained by plotting $R_{vv}(\theta) - (4/3)R_{vh}(\theta)$ versus k^2 . For brevity, we will designate the quantity $R_{vv} - (4/3)R_{vh}$ by Y. From the treatment of Utiyama²⁷

$$Y(\theta) = Kc\langle M \rangle_w[1 - \langle s^2 \rangle_z k^2/3] \quad (25)$$

while for the treatment of Nagai,²⁵ with the term in g_i neglected,

$$Y(\theta) = Kc\langle M \rangle_w[1 - (qL/9)(1 - 3/X - 4\epsilon/15X)k^2] \quad (26)$$

Two parameters, the length per repeating unit and the molecular weight per angstrom, are needed to treat the experimental results in terms of the wormlike chain model. From the calculations of Erman, Flory, and Hummel,²⁹ we obtain a length per repeating unit of 12.88 Å, and since the molecular weight per repeat is 316, the molecular weight per Å is $M_L = 24.53$ dalton/Å. From study of models of the repeating unit we expect the diameter of the chain to be between 10 and 15 Å.

The excess scattering was quite weak due to the small value of dn/dc , the long wavelength, and the rather low power of our He-Ne laser. Static light scattering data were only obtained for five fractions having intrinsic viscosities greater than 1.1 dL/g. Fractions having lower intrinsic viscosity gave such weak excess scattering that good Zimm plots could not be obtained. Two other fractions, F2 and F5, were not studied. As shown in Figure 6, ρ_v was mea-

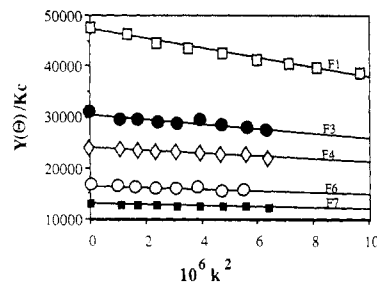


Figure 7. Plot for five fractions of $Y(\theta)/Kc$ versus k^2 according to eq 26.

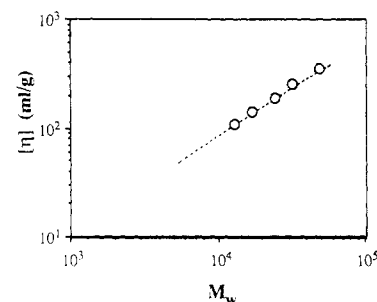


Figure 8. log-log plot of $[\eta]$ versus $\langle M \rangle_w$. The dashed curve represents the fit of the Yamakawa-Fujii treatment.

sured at each concentration and extrapolated to infinite dilution. The results are summarized in Table III. Figure 7 illustrates a plot of Y versus k^2 . The intercept gives $\langle M \rangle_w$ and the slope is equal to $\langle s^2 \rangle_z \langle M \rangle_w/3$. The corrected molecular weights obtained by the three methods are nearly the same. The corrected mean-square radius of gyration differs significantly, depending upon which correction is used, as can be seen in Table III. The functions f_1 and f_2 in the treatment of Berry²⁸ can be estimated from Figure 3 in his paper. Berry assumed f_1 and f_2 were unity because he was dealing with a highly chain-extended polymer. The apparent values of the second virial coefficient increase with increasing molecular weight, but after correction there does not appear to be any molecular weight dependence.

Figure 8 shows a log-log plot of the intrinsic viscosity, $[\eta]$ (dL/g), versus $\langle M \rangle_w$. The relation for this line is

$$[\eta] = 3 \times 10^{-4} \langle M \rangle_w^{0.869} \quad (27)$$

These data were fitted to the treatment of Yamakawa and Fujii.³⁰ The dashed line in Figure 8 indicates the fit obtained by using a persistence length of 60 Å and a chain diameter of 10 Å.

Bohdanecky's treatment³¹ offers another approach to determine the persistence length from $[\eta]$ and $\langle M \rangle_w$. His relations are

$$[\langle M \rangle_w^2/[\eta]]^{1/3} = A_n + B_n \langle M \rangle_w^{1/2} \quad (28)$$

$$A_n = A_0 M_L \Phi^{-1/3} \quad (29)$$

$$B_n = B_0 \Phi^{-1/3} (\langle r_0^2 \rangle / \langle M \rangle_w)^{1/2} \quad (30)$$

where

$$\langle r_0^2 \rangle / \langle M \rangle_w = 2q/M_L \quad (31)$$

$$A_0 = 0.46 - 0.53 \log(d/2q) \quad (32)$$

$$B_0 = 1.00 - 0.0367 \log(d/2q) \quad (33)$$

Here $\langle r_0^2 \rangle$ is the mean-square end-to-end distance of the chain, Φ is Flory's hydrodynamic constant, 2.87×10^{23} mol⁻¹, $2q$ is the length of a Kuhn segment, and d is the diameter of the polymer chain. Figure 9 shows a plot of

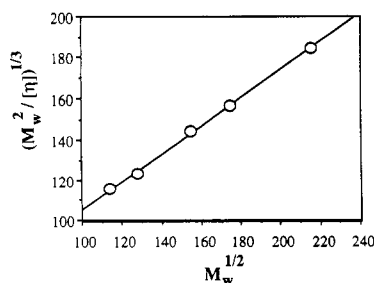


Figure 9. Plot of $(\langle M \rangle_w/[η])^{1/3}$ versus $\langle M \rangle_w^{1/2}$ according to Bohdanecký's treatment.

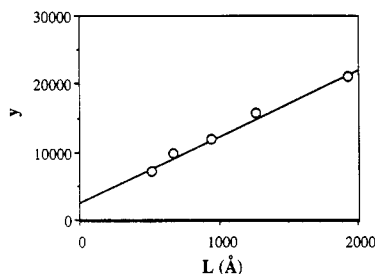


Figure 10. Values of y in eq 34 plotted against the contour length L according to the treatment of Ying and Chu.

$(\langle M \rangle_w/[η])^{1/3}$ versus $\langle M \rangle_w^{1/2}$ for this polymer. It gives a chain diameter of 16 Å and a Kuhn length of 123 Å. The latter value corresponds to a persistence length of 61 Å.

Ying and Chu³² have developed a method to calculate the persistence length by plotting $Y(θ)/Kc$ versus k^2 . The corrected molecular weight can be calculated from the intercept by using eq 25 and 26. Dividing the slope by $\langle M \rangle_w$ gives

$$y = qL/9 - y_0 \quad (34)$$

where

$$y_0 = (1/9)[3 + (4/5)\delta_0]q^2 \quad (35)$$

where ϵ is replaced by $3\delta_0$. Horn³³ has defined δ_0 as the intrinsic anisotropy of the scattering elements. His expression for δ_0 is

$$\delta_0 = \frac{(\alpha_1 - \alpha_2)^2 + (\alpha_1 - \alpha_3)^2 + (\alpha_2 - \alpha_3)^2}{2(\alpha_1 + \alpha_2 + \alpha_3)^2} \quad (36)$$

where the α_i are the principal polarizabilities of the scattering element. The slope of a plot of y versus L , as shown in Figure 10, is $q/9$. This yields a persistence length of 87 Å.

4. Dynamic Light Scattering. Before discussing the translational diffusion coefficient, the critical concentration for dilute polymer solutions needs to be defined. At the critical concentration, chains begin to overlap and entangle, so new dynamic processes come into play. For this reason the concentration dependence of the translational diffusion coefficient changes at the critical concentration. This was first observed by Mandelkern and Flory³⁴ for solutions of polystyrene. Adam and Delsanti³⁵ derived the following expression for the critical concentration, c^* :

$$c^* = \langle M \rangle_w / N_A \langle s^2 \rangle^{3/2} \quad (37)$$

Graessley³⁶ used the relation $\langle r_0^2 \rangle = 6\langle s_0^2 \rangle$ and Flory's hydrodynamic parameter Φ to obtain

$$c^* = \langle M \rangle_w / (8N_A \langle s^2 \rangle^{3/2}) \quad (38)$$

and

$$c^* = 6^{3/2}\Phi / (8N_A[\eta]) \quad (39)$$

Table IV
Values of the Critical Concentration $10^3 c^*$ (g/mL)

author	fraction				
	F1	F3	F4	F6	F7
Adam	20.02	28.97	36.63	49.14	62.94
Graessley	2.50	3.62	4.58	6.02	7.87
Han	4.78	6.92	8.75	11.49	15.02
Chu					
coil	10.89	15.77	19.94	26.20	34.26
wormlike	3.65	4.55	5.14	6.19	6.98
rod	0.030	0.074	0.120	0.252	0.406

Pecora and Han³⁷ have defined the critical concentration as

$$c^* = \langle M \rangle_w / (4\pi/3)N_A \langle s^2 \rangle^{3/2} \quad (40)$$

or

$$c^* = (3/4)(6^{3/2}\Phi/N_A[\eta]) \quad (41)$$

More recently Ying and Chu³⁸ have summarized relations for the critical concentration for various chain conformations:

$$c^*_{\text{coil}} = 8\langle M \rangle_w / (N_A \langle s_0^2 \rangle^{3/2}) \quad (42)$$

By use of the same approach as above, this can be transformed into

$$c^*_{\text{coil}} = 8\Phi / (N_A[\eta]) \quad (43)$$

For a wormlike chain they obtained

$$c^*_{\text{WL}} = 2^{3/2}\langle M \rangle_w / [N_A(qL)^{3/2}] \quad (44)$$

and for rods

$$c^*_{\text{rod}} = 2^{3/2}\langle M \rangle_w / (N_A L^3) \quad (45)$$

Values of c^* are summarized in Table IV for the case $q = 80$ Å and taking $\Phi = 2.87 \times 10^{23}$. The dynamic measurements were carried out by using concentrations below the critical concentrations in Table IV, except those for rods.

The correlation function, $G(x)$, is calculated from

$$G(x) = \lim_{T \rightarrow \infty} \frac{1}{2T} \int_{-T}^T I(t)I(t+x) dt \quad (46)$$

For a monodisperse sample, Ford⁴ relates the correlation function to the diffusion constant, D , as follows:

$$G(x) = 1 + 2f(n_{\text{coh}})(I_s/I_{\text{LO}}) \exp(-2Dk^2x) \quad (47)$$

where n_{coh} is the number of coherence areas, I_s is the intensity of the scattered light, I_{LO} is the intensity scattered by the local oscillator, and k is the reciprocal scattering vector.

In fact, even a polymer fraction is polydisperse, so that the correlation function for this case is given by Ying and Chu as³⁹

$$G(x) = 1 + b \exp[-Dk^2 + \sum_i (-1)^i \mu_i x^i / i!] \quad (48)$$

We analyzed the first and second cumulants using the least-square method.

The hydrodynamic radius, R_H , can be calculated from the translational diffusion coefficient by using the Stokes-Einstein relation

$$D = k_B T / (6\pi\eta_0 R_H) \quad (49)$$

where k_B is Boltzmann's constant and η_0 is the viscosity of the solvent. The correlation function might include a contribution to rotational motion,⁴⁰ but for our system rotation can be ignored because it is much faster than translational motion. For accurate results Dk^2 should be

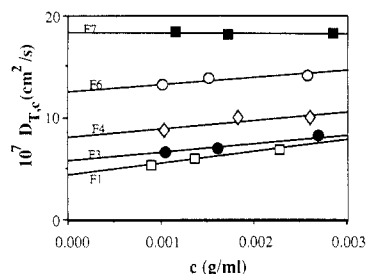


Figure 11. Concentration dependence of the translational diffusion coefficient, D_0 , for five fractions.

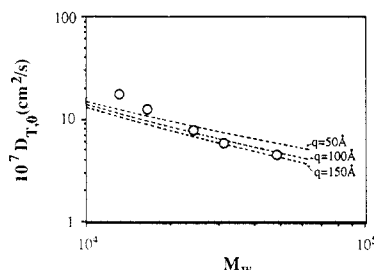


Figure 12. log-log plot of D_0 versus $\langle M \rangle_w$. The dashed curves represent values calculated according to the treatment of Yamakawa and Fujii for persistence lengths of 50, 100, and 150 Å.

Table V
Dynamic Light Scattering Results

	fraction				
	F1	F3	F4	F6	F7
$10^8 D_0$, cm ² /s	4.37	5.73	8.07	12.49	18.28
k_D , cm ³ /g	265.0	148.0	102.0	56.5	2.24

measured at several angles and plotted as a function of k^2 . However, in our system the scattering is so weak that it required over 12 h to develop the correlation function. Dk^2 was measured for fraction F4 at the angles 20°, 30°, and 40°. These data produced a linear relation, and the same slope was used to extrapolate data for the other fractions measured at a scattering angle of 20°.

For a dilute solution, the translational diffusion constant is a linear function of concentration:

$$D = D_0(1 + k_D c) \quad (50)$$

According to Pecora and Han,³⁷ k_D should be positive for polymers in good solvents. Figure 11 illustrates the concentration dependence of the translational diffusion coefficient. Values of D_0 and k_D are listed in Table V. The k_D values are positive and decrease with increasing molecular weight.

Figure 12 shows a log-log plot of D_0 (cm²/s) versus $\langle M \rangle_w$. The equation of the full line representing the limiting slope at high molecular weight is

$$D_0 = 1.8 \times 10^{-10} \langle M \rangle_w^{0.73} \quad (51)$$

The D_0 values for the two fractions of lowest molecular weight appear to be somewhat too large. Yamakawa and Fujii⁴³ have developed a treatment of the molecular weight dependence of D_0 . The dashed curves in Figure 12 indicate the results of these calculations. A persistence length of 150 Å and a diameter of 10 Å appear to offer the best representation of the data for fractions of higher molecular weight.

Values obtained by three methods for the persistence length of poly(phenylhydroquinone-*co*-terephthalic acid) are listed in Table VI. These range from 60 to 150 Å. If the two results calculated from the $[\eta]$ versus $\langle M \rangle_w$ are counted as a single entry, the average is 100 ± 34 Å.

Table VI
Values of the Persistence Length

data	method	q , Å
$[\eta]$, $\langle M \rangle_w$	Yamakawa-Fujii	60
	Bohdanecky	61
anisotropy	$R_{vv} - (4/3)R_{vh}$ (Chu)	87
D	Yamakawa-Fujii	150
		av 100 ± 34

Discussion

The limited range of solvents for wholly aromatic polyesters makes light scattering measurements difficult. We selected a binary solvent system, *o*-dichlorobenzene and *p*-chlorophenol, because these liquids have nearly the same refractive index. Unfortunately, the refractive index increment is rather small. This fact, coupled with the need to use longer wavelength light to avoid absorbance and the low power of our He-Ne laser, made it difficult to perform light scattering measurements for this system.

Erman, Flory, and Hummel²⁹ have calculated a persistence length, q , of 785 Å for poly(hydroquinone-*co*-terephthalic acid). The same authors obtained $q = 422$ Å for poly(*p*-phenylenediamine-*co*-terephthalic acid). The experimental values of Arpin and Strazielle^{3,4} for the latter polymer range from 150 to 200 Å while a more recent determination of Ying et al.⁶ gave $q = 290$ Å. The value $q = 650$ Å reported from flow birefringence measurements by Tsvetkov and Shtennikova⁵ is well beyond the error of the other experimental values.

Erman, Flory, and Hummel²⁹ state that their calculated values of the persistence length should be regarded as upper limits and perhaps should be reduced by 25–40%. A 40% reduction would bring the persistence length of poly(*p*-phenylenediamine-*co*-terephthalic acid) to 250 Å, which stands in reasonable agreement with the experimental values cited above. A similar reduction would yield $q = 470$ Å for poly(hydroquinone-*co*-terephthalic acid). Comparison with the value 100 Å obtained in the present work indicates that a pendent phenyl group on hydroquinone significantly reduces the unperturbed dimensions of this polymer. Examination of space-filling models indicates that the carbonyl group adjacent to the pendent phenyl ring must be displaced from the plane of the benzene ring. This would destroy the partial double bond in that carbonyl group, leading to a more flexible chain.

If one assumes that the diameter of poly(phenylhydroquinone-*co*-terephthalic acid) is 12 Å, then the axial ratio of the Kuhn link $\zeta = 2q/d$, is 16.7 at 25 °C. We⁴² have pointed out that a Kuhn chain polymer can undergo a thermotropic nematic–isotropic transition if the unperturbed dimensions are temperature dependent. The transition occurs at the temperature which reduces ζ to 6.70. For two polymers, poly(hexyl isocyanate)⁴² (PHIC) and (hydroxypropyl)cellulose⁴³ (HPC) the values of ζ extrapolated to $T/T_{NI} = 1.0$ are very close to 6.7.⁴² The polymer studied here is closest to HPC, for which $q = 100$ Å at 25 °C and $d \ln \zeta / dT = -5 \times 10^{-3}$. However, T_{NI} is only 210 °C for HPC, while it is 450 °C for the present polymer. If $\zeta = 6.70$ at 450 °C, then $d \ln \zeta / dT$ must be -2.1×10^{-3} for poly(phenylhydroquinone-*co*-terephthalic acid). This value is smaller in magnitude than expected.

Acknowledgment. We express our appreciation to the National Science Foundation for support of this work by Grant DMR-8419803. We also thank Unitika Ltd. for a stipend which supported T.T. during the course of this work.

Registry No. (Terephthalic acid)(phenylhydroquinone diacetate) (copolymer), 67203-16-1; (terephthalic acid)(phenyl-

hydroquinone diacetate) (SRU), 67256-36-4.

References and Notes

- (1) Payet, C. R. U.S. Patent 4 159 365, 1979.
- (2) Kratky, O.; Porod, G. *Recl. Trav. Chim. Pays-Bas* **1949**, *68*, 1106.
- (3) Arpin, M.; Strazielle, C. *Macromol. Chem.* **1976**, *177*, 581, 585.
- (4) Arpin, M.; Strazielle, C. *Polymer* **1977**, *18*, 262, 591.
- (5) Tsvetkov, V. N.; Shtennikova, I. N. *Macromolecules* **1978**, *11*, 306.
- (6) Ying, A.; Chu, B.; Qian, R.; Bao, J.; Zhang, J.; Xu, C. *Polymer* **1985**, *26*, 1401.
- (7) Bianchi, E.; Ciferri, A.; Tealdi, A.; Krigbaum, W. R. *J. Polym. Sci. Polym. Phys. Ed.* **1979**, *17*, 2091.
- (8) Bianchi, E.; Ciferri, A.; Preston, J.; Krigbaum, W. R. *J. Polym. Sci., Polym. Phys. Ed.* **1981**, *19*, 863.
- (9) Krigbaum, W. R.; Sasaki, S. *J. Polym. Sci., Polym. Phys. Ed.* **1981**, *19*, 1339.
- (10) Tsvetkov, V. N.; Tsepelevich, S. O. *Eur. Polym. J.* **1983**, *19*, 267.
- (11) Sakurai, K.; Ochi, K.; Norisue, T.; Fujita, H. *Polym. J.* **1984**, *16*, 559.
- (12) Saito, M. *Polym. J.* **1983**, *15*, 213.
- (13) Schmidt, M. *Macromolecules* **1984**, *17*, 553.
- (14) Kubota, K.; Tominga, Y.; Fujima, S. *Macromolecules* **1986**, *19*, 1604.
- (15) Jackson, W., Jr. *Br. Polym. J.* **1980**, *12*, 154.
- (16) Luise, R. R. U.S. Patent 4 183 895, 1980.
- (17) Lenz, R. In *Recent Advances in Liquid Crystalline Polymers*; Chapoy, L. L., Ed.; Elsevier Applied Science Publishers: New York, 1983; Chapter 1.
- (18) Brice, B. A.; Halwer, M. *J. Opt. Soc. Am.* **1951**, *41*, 1033.
- (19) Ford, N. C. In *Dynamic Light Scattering*; Pecora, R., Ed.; Plenum: New York, 1986; Chapter 2.
- (20) Chu, B. *Laser Light Scattering*; Academic: New York, 1985; Chapter 7.
- (21) Krigbaum, W. R.; Hakemi, H.; Kotek, R. *Macromolecules* **1985**, *18*, 965.
- (22) Utiyama, H. In *Light Scattering from Polymer Solutions*; Huglin, M. B., Ed.; Academic: New York, 1972; p 61.
- (23) Kaye, W.; Havlik, H. *J. Appl. Opt.* **1977**, *12*, 541.
- (24) Pike, E. R.; Pomeroy, W. R. M.; Vaghan, J. M. *J. Chem. Phys.* **1975**, *62*, 3188.
- (25) Nagai, K. *Polym. J.* **1972**, *3*, 67.
- (26) Zimm, B. H. *J. Chem. Phys.* **1948**, *16*, 1099.
- (27) Utiyama, H. In *Modern Theory of Polymer Solutions*; Yamakawa, H., Ed.; Harper and Row: New York, 1971.
- (28) Berry, G. C. *J. Polym. Sci., Polym. Symp.* **1978**, *65*, 143.
- (29) Erman, B.; Flory, P. J.; Hummel, J. P. *Macromolecules* **1980**, *13*, 484.
- (30) Yamakawa, H.; Fujii, M. *Macromolecules* **1974**, *7*, 128.
- (31) Bohdanecky, M. *Macromolecules* **1983**, *16*, 1483.
- (32) Ying, Q.; Chu, B. *Makromol. Chem., Rapid Commun.* **1985**, *5*, 938.
- (33) Horn, P. *Ann. Phys.* **1955**, *10*, 386.
- (34) Mandelkern, L.; Flory, P. J. *J. Chem. Phys.* **1951**, *19*, 984.
- (35) Adam, M.; Delsanti, M. *Macromolecules* **1977**, *10*, 1229.
- (36) Graessley, M. *Polymer* **1980**, *21*, 258.
- (37) Pecora, R.; Han, C. C. *Dynamic Light Scattering*; Plenum: New York, 1985; Chapter 5.
- (38) Ying, Q.; Chu, B. *Macromolecules* **1987**, *20*, 362.
- (39) Ying, Q.; Chu, B. *Macromolecules* **1986**, *19*, 1580.
- (40) Zero, K. *Dynamic Light Scattering*; Pecora, R., Ed.; Plenum: New York, 1985; Chapter 3.
- (41) Yamakawa, H.; Fujii, M. *Macromolecules* **1973**, *6*, 497.
- (42) Krigbaum, W. R.; Hakemi, H.; Ciferri, A.; Conio, G. *Macromolecules* **1985**, *18*, 973.
- (43) Aden, M. A.; Bianchi, E.; Ciferri, A.; Conio, G.; Tealdi, A. *Macromolecules* **1984**, *17*, 2010.

Monolayer of Polystyrene Monomolecular Particles on a Water Surface Studied by Langmuir-Type Film Balance and Transmission Electron Microscopy^{†,1}

Jiro Kumaki[‡]

Research Development Corporation of Japan, c/o Department of Chemistry, Faculty of Science and Technology, Sophia University, Kioicho, Chiyoda-ku, Tokyo 102, Japan.
Received March 9, 1987; Revised Manuscript Received August 19, 1987

ABSTRACT: The behavior of a monolayer of polystyrene monomolecular particles which was obtained by spreading dilute solutions in benzene on the water surface was studied by a Langmuir-type film balance and transmission electron microscopy (TEM). Since polystyrene has no hydrophilic group, the surface pressure measured by the film balance was not due to the real decrease of the surface tension but due to a mechanical force by compression, thus the π -A curves were apparent π -A curves. However, the macroscopic observation by the film balance was in good agreement with the microscopic observation by TEM, indicating the particles are stable against the compression. At the limiting area, A_0 , the monomolecular particles covered 56% of the water surface, but they could not be most closely packed by further compression. In addition to the higher molecular weight samples, apparent π -A curves were measured for lower molecular weight samples, for which formation of monomolecular particles has not been confirmed because of the limited resolution of TEM; the observed small A_0 indicated the particles were not formed or were unstable against the compression.

I. Introduction

Polymer monolayers that are spread on the water surface have been widely studied, including both synthetic polymers and biopolymers.²⁻⁴ Polymers with sufficient hydrophilic groups in the repeating unit, such as poly(vinyl acetate),⁵ are well-known to be ideal monolayers on the water surface with every repeating unit being absorbed on the water surface.

In contrast polymers without hydrophilic groups in the repeating unit, such as polystyrene⁶⁻⁸ and poly(vinyl chloride),³ do not spread to be monolayers on the water surface because of the lack of the sufficient affinity to water. The surface pressure-area curves (π -A curves) of these polymers show extraordinarily small limiting areas compared with their molecular structures, indicating the polymers exist on the water surface as flakes or multilayers. Recently we studied polystyrene spread films on the water surface from dilute solutions in benzene by transmission electron microscopy (TEM) and found that if the concentration of the solution is dilute enough (about 2×10^{-6} g/mL), polystyrene monomolecular particles, each of which contains one molecule, were obtained on the water surface.⁹

[†] Presented in part before the 35th Annual Symposium of Polymer Science, Society of Polymer Science, Japan, Dec 1986. Kumaki J. *Polym. Prepr. Jpn.* **1986**, *35*, 3544-3547.

[‡] Present address: Polymers Research Laboratories, Toray Industries Inc., Sonoyama, Ohtsu, Shiga 520, Japan.